Effects of Sensor Resolution and Localization Rate on the Performance of a Myokinetic Control Interface

Federico Masiero, Edoardo Sinibaldi, *Member, IEEE*, Francesco Clemente, and Christian Cipriani, *Senior Member, IEEE*

***Abstract*—Magnetic tracking systems have been widely investigated in biomedical engineering due to the transparency of the human body to static magnetic fields. We recently proposed a novel human-machine interface for prosthetic application, namely the myokinetic interface. This controls multi-articulated prostheses by tracking magnets implanted in the residual muscles of individuals with amputation. Previous studies in this area focused solely on the choice and tuning of the localization algorithm. Here, we addressed the role of the intrinsic properties of the sensors, by analysing their effects on the tracking accuracy and on the computation time of the localization algorithm, through experimentally-verified computer simulations. We observed that the tracking accuracy is primarily affected by the localization rate, which is directly related to the sampling frequency of the sensors, and less significantly affected by the sensor resolution. The computation time, instead, proved positively correlated to the number of MMs, and negatively correlated with the localization rate. Our results may contribute to the development of novel human-machine interfaces for prosthetic limbs and could be extended to a broad range of applications involving magnetic tracking.**

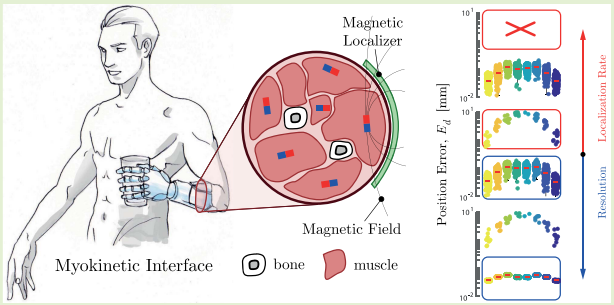

***Index Terms*—Human-machine interface, magnetic field, magnetic tracking, myokinetic interface, sensor selection, upper limb prosthetics.**

I. Introduction

MAGNETIC tracking systems have been widely investigated in biomedical engineering. Indeed, the transparency of the human body to low-frequency magnetic fields and the unnecessity of a free line-of-sight between the magnetic target and the tracker make such systems attractive candidates for intra-body applications [1], [2].

Magnetic tracking is the problem of reconstructing the position and orientation (namely, the *pose*) of one or multiple magnetic sources by measuring their field with an appropriate number of sensors. Magnetic tracking systems exploit either static fields [3] (generated by permanent magnets) or low-frequency alternating fields [4] (generated by electromagnets or coils). One of the main advantages when tracking permanent magnets, rather than coils, is that they are passive, and thus they neither require a power supply nor wiring. Hence, permanent magnets represent an optimal candidate solution when attempting to track an implanted device.

Most of the literature concerning magnetic tracking in biomedical devices is confined to single-objective (i.e., single-source) tracking. Examples of single-objective *trackers* have been devised for navigating endoscopic capsules inside the gastrointestinal tract [5]–[8], improving the guidance of ventriculostomy interventions [9], as well as controlling magnetic catheters, [10], [11]. However, some biomedical applications require the simultaneous localization of multiple sources, like magnetic drug delivery or navigation of multiple medical instruments [12].

Among the multi-objective magnetic trackers lies the concept of a new human-machine interface (HMI) to control prosthetic limbs recently proposed by our group and named the *myokinetic control* interface [13]. In short, magnetic markers,

Manuscript received July 12, 2021; accepted August 25, 2021. Date of publication September 3, 2021; date of current version October 18, 2021. This work was supported by the European Research Council through the Bidirectional MyoKinetic Implanted Interface for Natural Control of Artificial Limbs (MYKI) Project under Grant ERC-2015-StG and Grant 679820. The associate editor coordinating the review of this article and approving it for publication was Prof. Tien-Kan Chung. *(Corresponding authors: Federico Masiero; Edoardo Sinibaldi.)*

Federico Masiero, Francesco Clemente, and Christian Cipriani are with the Biorobotics Institute, Scuola Superiore Sant'Anna, 56127 Pisa, Italy, and also with the Department of Excellence in Robotics and AI, Scuola Superiore Sant'Anna, 56127 Pisa, Italy (e-mail: federico.masiero@santannapisa.it).

Edoardo Sinibaldi is with the Center for Micro-BioRobotics@SSSA, Istituto Italiano di Tecnologia, 16163 Genoa, Italy (e-mail: edoardo.sinibaldi@iit.it).

Digital Object Identifier 10.1109/JSEN.2021.3109870

MMs (e.g., permanent magnets), implanted in the residual muscles of an individual with limb amputation, could be tracked to retrieve the contractions/elongations of such muscles. The information of the muscles' displacements could be used to implement direct control over the corresponding degrees of freedom (DoFs) in an artificial limb, like a robotic hand. Ideally, by tracking multiple MMs, such a system could allow simultaneous and independent control of the DoFs of the prosthesis, restoring a close to natural control.

Representative multi-objective magnetic trackers were described by Yang *et al.* [14], Taylor *et al.* [15], and Tarantino *et al.* [16], which demonstrated systems capable of localizing up to three, four, and seven MMs, respectively. All of them used model-based optimization approaches to retrieve the poses of the magnets, using the well-known point dipole model [17]. Hitherto, this approach has proven to be the fastest and the most accurate [15], [18]. Moreover, it was shown that the viability of such an approach depends on several factors, including the number and arrangement of the MMs [15], [19], [20], the volume of the workspace w.r.t. the strength of the magnetic field produced by the MMs [21], the approximations used in the point dipole model [17], [22], the cost-function and the numerical solver used [18], [23], and several other environmental factors [13]. Nonetheless, most of these findings were confined to single-objective tracking. Hence, generalizing the outcomes to multiple sources represents a significant contribution towards the understanding of the underlying phenomena that can lead to the improvement of state-of-the-art magnetic trackers.

In addition, very few studies investigated the role of the sensory system for magnetic tracking. While the effects of the number and spatial distribution of the sensors were seldom investigated [24]–[28], the effects of the intrinsic properties of the sensors were largely overlooked. Among them, the resolution and the sampling frequency are arguably the most important ones aiming to localize a target with high accuracy and bandwidth. Nonetheless, considering that in magnetic tracking the sampling and the computation phases cannot be disentangled (pretty much like the sampling and conversion phases in an ADC), it is the *localization rate* that deserves to be investigated (rather than the sampling frequency alone).

Thus, taking our previous study as a starting point [20], here we investigated how sensor resolution and rate of the localization process affect the localization error and the computation time in a multi-magnet localization problem. For this purpose, we simulated their effects on a representative, yet generalizable, localization scenario with a planar sensor arrangement that resembled the unfolded geometry of the human forearm (in our application). We considered sensor resolutions with three different orders of magnitude (0.1 mG, 1 mG, and 10 mG), according to values exhibited by commercial miniaturized magnetic sensors. We assessed our findings by means of two metrics: the position error and the number of iterations of the Levenberg Marquardt algorithm (LMA). We observed that sensor resolution plays a minor role in the accuracy of the localization, while the localization rate dramatically affects its performance, reducing exponentially the capability of retrieving the poses of all the MMs. Finally, to verify/assess the significance of our outcomes, the simulated localization errors were compared with those achieved with a physical system employing 32 tri-axial magnetic sensors.

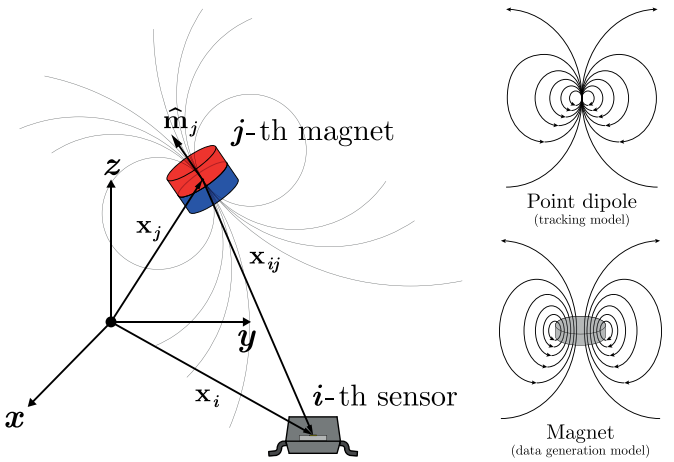

Fig. 1. The coordinate system for modelling point dipoles.

These outcomes represent a further advancement towards the implementation of a myokinetic HMI but can be of interest for several bioengineering applications in which the tracking of multiple MMs is required.

II. Materials and Methods

A. Mathematical Framework

We used the point dipole model approximation in order to simplify the solution of the localization problem akin to our previous studies [13], [16], [29]. This model approximates each MM as a point magnetic dipole located at its centre. Thus, the magnetic field $\mathbf{B}(\mathbf{x}_i)$, generated at the location $\mathbf{x}_i$ by N_m dipoles, located at $\mathbf{x}_j$, $j = 1, \ldots, N_m$, with magnetic moment equal to $M_j \hat{\mathbf{m}}_j$ (here M_j and $\hat{\mathbf{m}}_j$ are the magnitude and direction of the magnetic moment of the j-th MM) can be computed as:

$$\mathbf{B}(\mathbf{x}_i) = \sum_{j=1}^{N_m} \frac{M_j \mu_r \mu_0}{4\pi} \left(\frac{3\left(\hat{\mathbf{m}}_j \cdot \mathbf{x}_{ij}\right)\mathbf{x}_{ij}}{\|\mathbf{x}_{ij}\|^5} - \frac{\hat{\mathbf{m}}_j}{\|\mathbf{x}_{ij}\|^3} \right), \quad (1)$$

where $\mathbf{x}_{ij} = \mathbf{x}_i - \mathbf{x}_j$ and $\mathbf{x}_i$ represent the relative locations of N_s sites where the magnetic field is measured (sensor locations, Fig. 1).

Measuring the compound magnetic field, generated by the N_m MMs, using N_s sensors, allows to solve Eq. (1) in favour of $\mathbf{x}_{ij}$, providing the solution to the localization problem and thus the input data required for the myokinetic control interface. However, as there is no closed-form solution (for more than one MM, [30]), the latter can only be obtained by numerical approximation.

In this work, we used MATLAB (R2019b, MathWorks, Natick, MA) to simulate the magnetic field generated by a number of MMs in space, as well as for tracking their poses (namely, the *direct* and *inverse* problems of magnetostatics, respectively). For the direct problem, we adopted the analytical model for axially magnetized cylindrical magnets, proposed in [31]. For the inverse problem, instead, the field sampled at

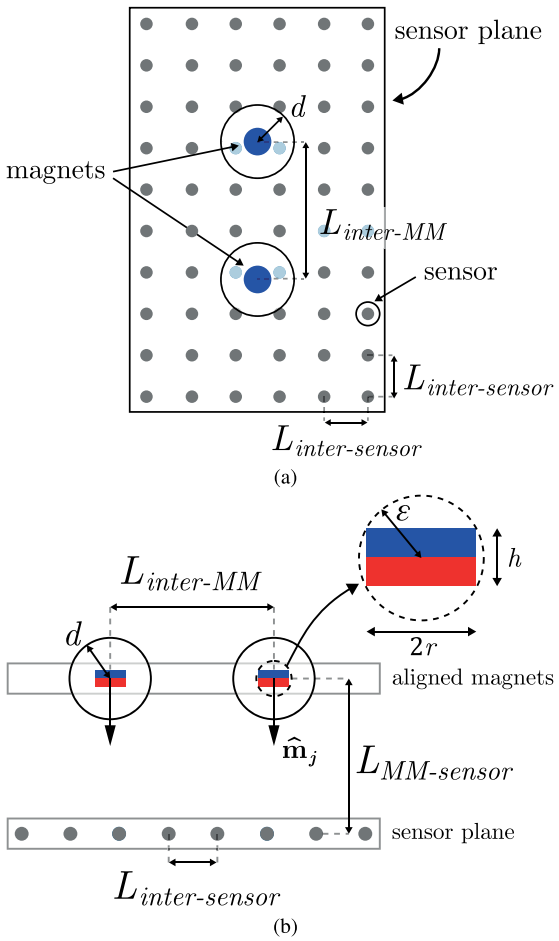

Fig. 2. Simulated setup. (a) Top view. (b) Lateral view. ε refers to the radius of the smallest sphere surrounding the MM.

N_s locations was fed to the lsqnonlin solver (implementing LMA [32]) to solve Eq. (1) offline, akin to our previous studies [13], [16], [29].

Different setups, mixing number of MMs, distance from the sensor-plane, resolution, and localization rate, were simulated in order to assess the localization errors.

All simulations were run on a desktop PC with an Intel i7-9750 2.60 GHz CPU, 16 GB of RAM, and Windows 10.

B. Simulation Setup

The simulated setup consisted of N_m equidistant MMs (MM_1−MM_{10}, at $L_{inter-MM}$ millimetres one from another) aligned, and placed at a distance $L_{MM-sensor}$ from a sensing surface/plane (Fig. 2). N_m ranged from 1 to 10, and each case identified a *test scenario*; thus, ten test scenarios were simulated. The MMs were modelled as NdFeB disc magnets ($r = h = 2$ mm) with the magnetization vector oriented towards the sensing plane (Fig. 2b). To investigate the effects of the sensor resolution and localization rate on the localization performance, in a general yet realistic manner, the sensing plane included sensors uniformly distributed on a planar grid (60 columns and 10 rows), with an inter-sensor distance ($L_{inter-sensor}$) of 9 mm. The latter was chosen as it is compatible with the distance allowed by commercial three-axis magnetic field sensors [29]. For each test scenario, we varied

TABLE I
SUMMARY OF THE SIMULATION PARAMETERS

Simulation Parameter	Value
Number of trials per condition	1000
Number of MMs	$1-10$
Number of sensors	600 (10×60 grid)
Initial condition distance, d	$0.8-5$ mm (step of 0.2 mm)
Sensor-magnet dist., $L_{MM-sensor}$	$10-50$ mm (step of 5 mm)
Inter-sensor dist., $L_{inter-sensor}$	9 mm
Inter-magnet dist., $L_{inter-MM}$	$L_{MM-sensor}$
Sensor resolution	0.1, 1, 10 mG
Sensor noise	rms = 0.5·resolution
Type of MM	Axial cylinder
Residual Flux Density	1.2706 T

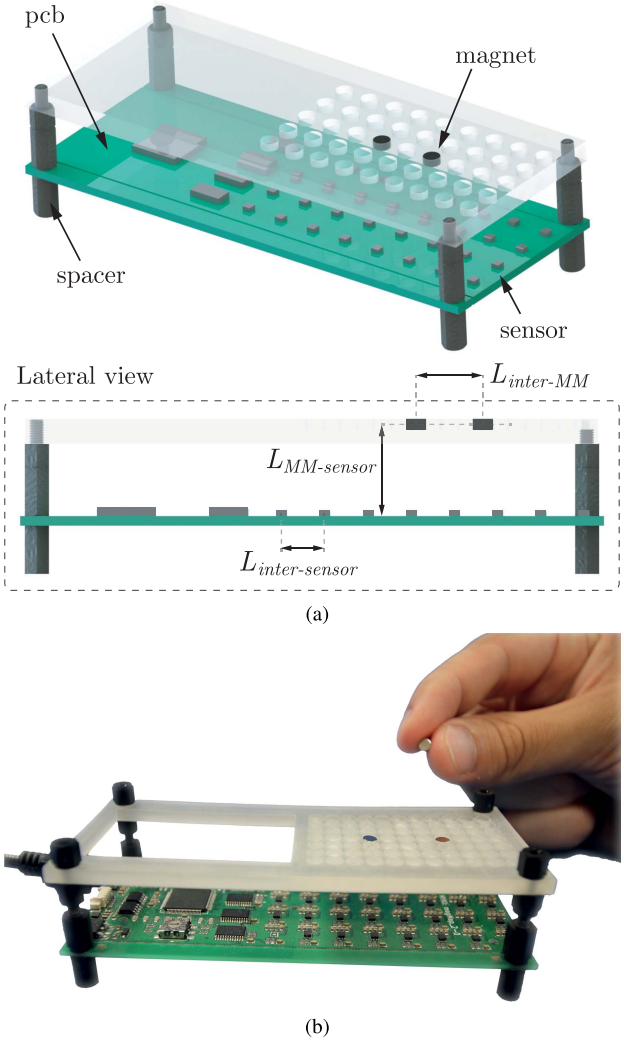

Fig. 3. Rendering (a) and picture (b) of the experimental setup.

$L_{MM-sensor}$ from 10 mm to 50 mm with a step of 5 mm. Besides, $L_{inter-MM}$ varied accordingly, keeping fixed the ratio $L_{inter-MM}/L_{MM-sensor} = 1$, in order to satisfy the rule identified in our previous study [20].

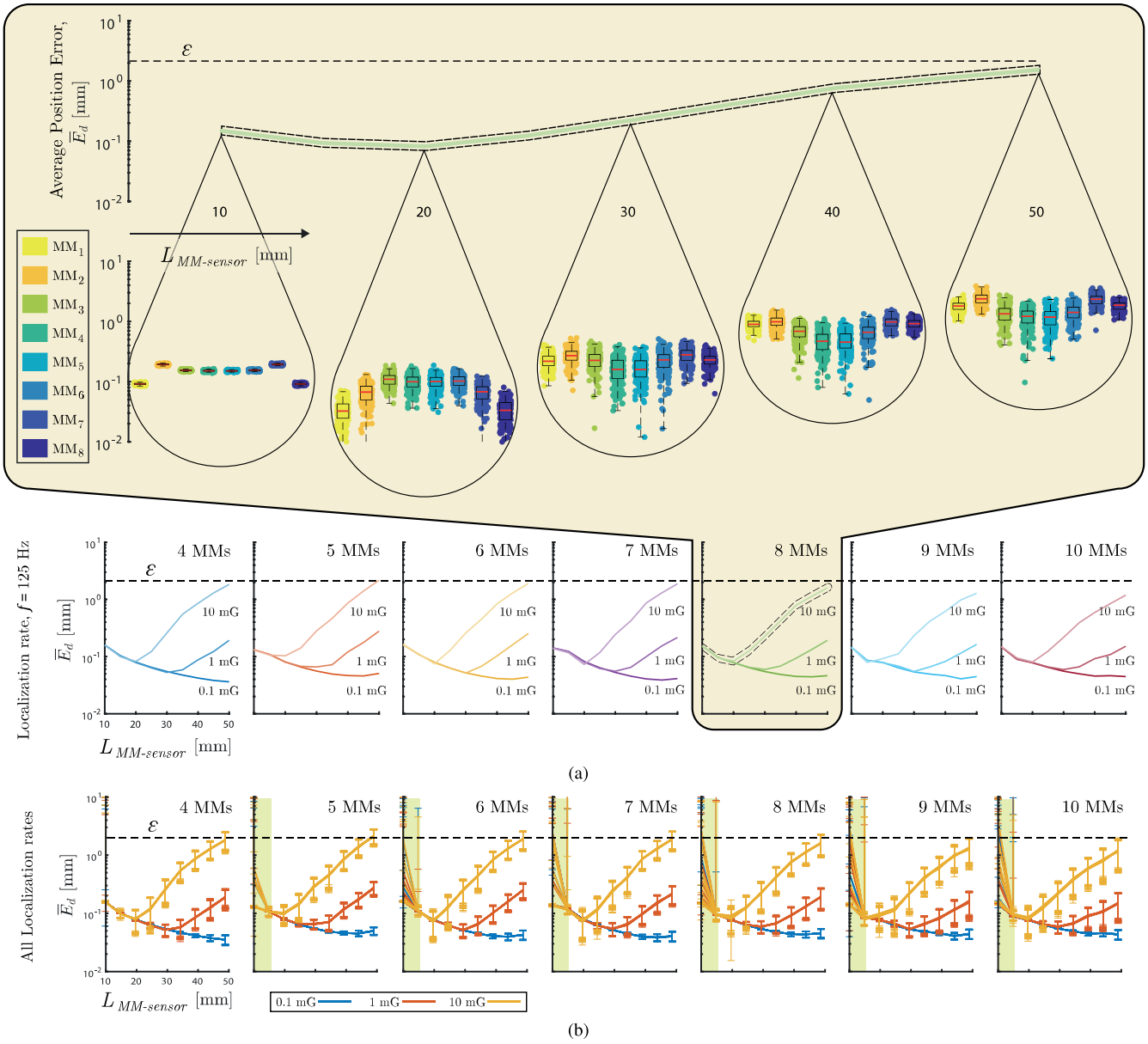

Fig. 4. The average position error, $\bar{E}_d$, vs. $L_{MM\text{-}sensor}$ for different localization rates showed a minimum. (a) The trend for 125 Hz localization rate, 8-MMs and 10 mG resolution; the minimum of $\bar{E}_d$ was reached for $L_{MM\text{-}sensor} = 20$ mm. (b) The trends across localization rates show high repeatability at all $L_{MM\text{-}sensor}$ with the exception of $L_{MM\text{-}sensor} = 10$ mm.

To study the effect of the resolution of the readings in the performance of the tracking, the LMA was fed with sensory data truncated at three degrees of resolution: 0.1 mG, 1 mG, 10 mG. This tested a very wide range: in fact, state-of-art miniaturized sensors exhibit a resolution spanning from 0.1 to 5 mG. Notably, before truncation, the readings were also perturbed with white Gaussian noise at a sub-resolution level (i.e., rms of 0.5·resolution), in order to account for the precision (repeatability) of the readings, and thus to produce more realistic results. The effect of the localization rate instead, was simulated by feeding the LMA with sensory data corresponding to magnets having travelled increasing distances, d. This described the case of magnets moving at a constant speed (or, equivalently, muscles contracting at a fixed phase) and sampled at varying frequencies. In detail, calling $\mathbf{x}_j$ the actual position of the j-th MM, and $\mathbf{x}_j^0$ the initial position fed to the LMA, we set 1000 initial conditions such that:

$$\|\mathbf{x}_j - \mathbf{x}_j^0\| = d\,, \quad \forall\, j = 1, \ldots, N_m, \tag{2}$$

where d ranged from 0.8 mm to 5 mm with a step of 0.2 mm (22 values). Satisfying Eq. (2) for each magnet, meant placing the initial guess for the LMA on the surface of a sphere centred in the barycentre of the MM with radius d, and with an arbitrary orientation (Fig. 2). Considering the worst case of muscles contracting at their fastest phase ($v = 10$ cm/s [33]) this corresponded to a simulated localization rate, f, ranging from 125 Hz ($d = 0.8$ mm) to 20 Hz ($d = 5$ mm), following:

$$f = \frac{v}{\|\mathbf{x}_j - \mathbf{x}_j^0\|} = \frac{v}{d}. \tag{3}$$

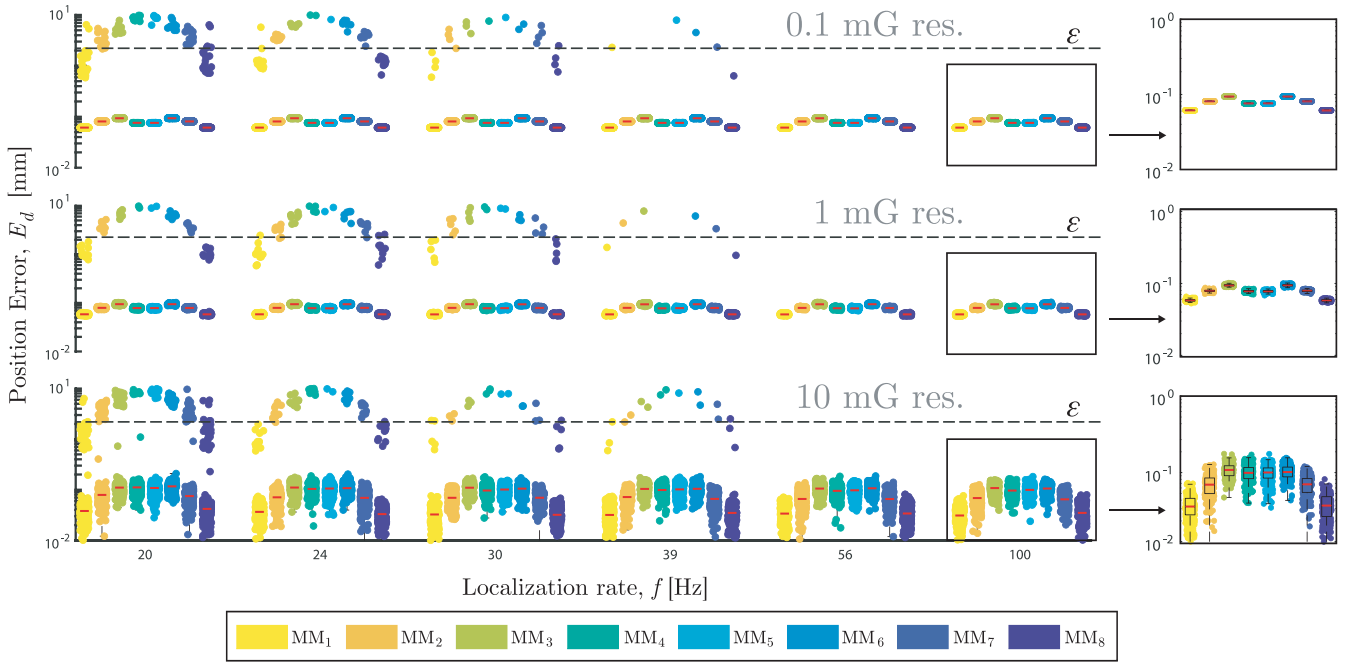

Fig. 5. Distribution of E_d vs. localization rate for each MM in case of 8-MMs tracking and $L_{MM\text{-}sensor} = 20$ mm. The spread of the distributions increases for rougher values of the resolution. Increasing values of the localization rate turn the distributions from bimodal to unimodal.

In summary, each test scenario was tested for nine heights of the magnets from the sensor plane, three degrees of resolution of the sensors, and 22 localization rates. The combination of all the parameters resulted in thousands of simulations (Table I).

C. Experimental Assessment

To verify the quality of our simulations, we compared the localization accuracy achieved with simulated and experimentally recorded data, using a physical demonstrator with a representative number of magnets and sensors.

A planar printed circuit board with 32 three-axis digital magnetometers (MAG3110, NXP Semiconductors NV, Eindhoven, Netherlands; full-scale output of ± 10 G and resolution of 1 mG), in an 8×4 rectangular grid ($L_{inter-sensor} = 9$ mm) was used to collect the magnetic field generated by NdFeB axially magnetized cylindrical MMs (N35, $r = h = 2$ mm). Different numbers of MMs (from 1 to 5; $L_{inter-MM}$ of 14 mm) were hold on a custom support with their magnetization vectors perpendicular to the sensor surface ($L_{MM-sensor} = 18.5$ mm) (Fig. 3). The MMs were kept steady in their positions, and 100 readings were recorded, for each number of MMs. We assessed the effects of the localization rate on the localization accuracy as for the simulated setup, i.e., by placing the initial condition of the LMA at a certain distance and random orientation w.r.t. their actual poses. Specifically, the selected distances were the same adopted also in the simulations to achieve the desired range of the localization rate (according to Eq. (3)).

The same physical setup was reproduced in simulation, for comparison. Notably, random Gaussian noise, with a standard deviation of 4 mG (corresponding to the noise characteristics exhibited by the physical sensors used) was added to the sampled simulated magnetic field. Finally, the localization accuracy of the physical and simulated setups was computed.

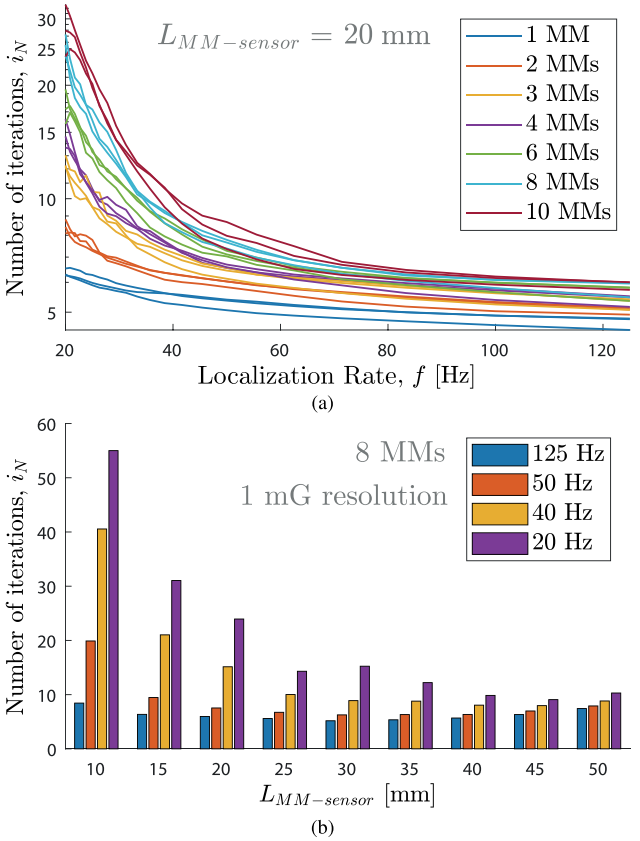

Fig. 6. (a) Number of iterations vs. the localization rate for the three resolutions. (b) Number of iterations vs $L_{MM\text{-}sensor}$ for four localizations rates (125, 50, 40, 20 Hz) in 8-MMs tracking.

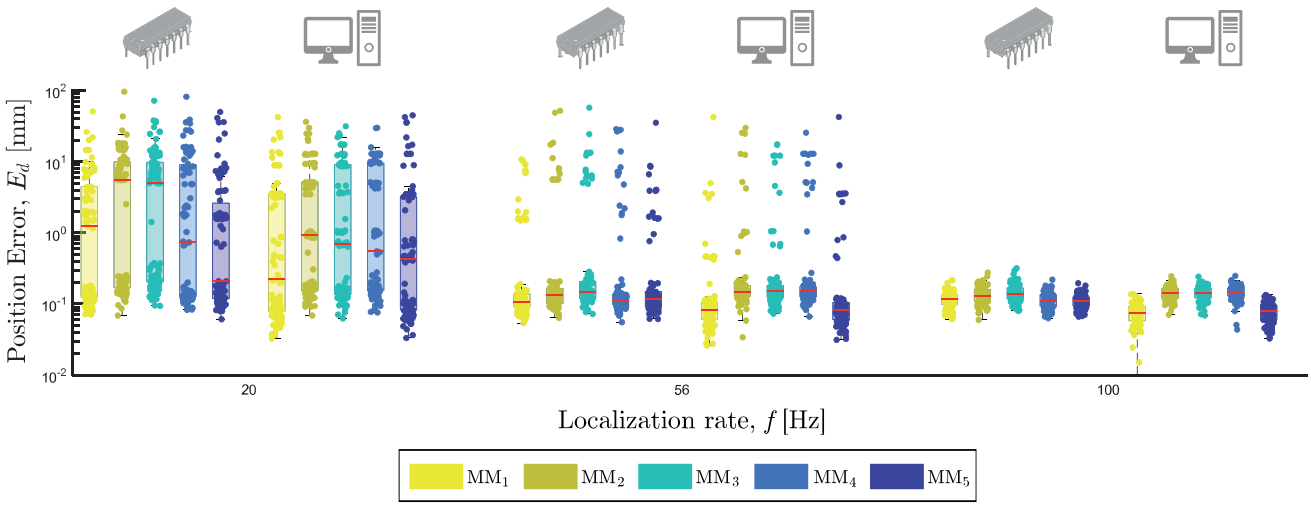

Fig. 7. Distribution of E_d vs. localization rate for each MM in the case of 5-MMs tracking (each box plot consisting of a 100 trials) for both experimental (left columns) and simulated (right columns) data.

D. Performance Metrics

The accuracy of the multi-magnet localizer was quantified by means of its position displacement error, E_d, i.e., the Euclidean distance between the estimated and actual positions of the MMs [18]. In particular, to understand the effects of the sensor resolution and localization rate on the accuracy and precision (or dispersion) of the localization algorithm, we analyzed the distribution of the E_d w.r.t. the simulation parameters. In addition, keeping the same settings of the solver (i.e., the default ones), the number of iterations required by the LMA to converge on a solution, i_N, was retrieved to infer the computation time needed to track the MMs.

III. Results

The profile of the average E_d, $\bar{E}_d$, showed a minimum w.r.t. the distance $L_{MM-sensor}$, which was dependent on the resolution of the sensors: better resolutions shifted the minimum of the curve towards larger distances $L_{MM-sensor}$ (Fig. 4a). For example, with 8-MMs, a localization rate of 125 Hz and a resolution of 10 mG, the $\bar{E}_d$ exhibited its minimum for $L_{MM-sensor}$ equal to 20 mm. Such minimum shifted to 30 mm and 40 mm with resolutions of 1 mG and 0.1 mG, respectively (Fig. 4a). The same behaviour was observed throughout all localization rates.

Interestingly, for $L_{MM-sensor}$ equal to 10 mm and the number of MMs greater than four, $\bar{E}_d$ proved dependent on the localization rate, demonstrating an increased variability w.r.t. larger distances (Fig. 4b). This proved true throughout all resolutions. Nonetheless, $\bar{E}_d$ was always smaller than its characteristic dimension (namely the radius ε of the smallest magnet bounding sphere) when changing the resolution, regardless the localization rate (Fig. 4b). A larger $\bar{E}_d$ variability could also be observed for increasing number of MMs (Fig. 4b).

By fixing the $L_{MM-sensor}$ and computing the E_d for each of the tracked MMs we observed somewhat bimodal distributions for the lower localization rates, and unimodal distributions for the larger ones, for all the magnets (Fig. 5 for $L_{MM-sensor} = 20$; the same result was found for all values of $L_{MM-sensor}$). This feature (unimodal/bimodal) proved consistent independently of the degree of resolution. A closer analysis on these additional lobes revealed that they were originated either when the localization algorithm swapped two neighbouring MMs (and thus, the position error E_d corresponds to the distance between them), or when the MMs were localized in-between two neighbouring MMs.

Also, the variability of the distribution proved consistent across the localization rate. In particular, the variability was related to the degree of the resolution, which influenced the precision of the localization by yielding to smaller variability of the lobes of E_d with better resolutions.

The number of iterations of the LMA, i_N, proved positively correlated to the number of MMs (Fig. 6a), and negatively correlated with the localization rate (Fig. 6b). For instance, with 8-MMs tracking, $L_{MM-sensor} = 20$ mm and 1 mG of resolution, i_N proved around 25 and 7 for 20 Hz and 125 Hz, respectively (Fig. 6a). Conversely, once fixed the other variables, i_N proved independent of the resolution. The trend between i_N and $L_{MM-sensor}$ instead showed a minimum (Fig. 6b).

An evidence of the quality of all these outcomes was provided by the comparison with the physical setup (Fig. 3). In fact, the localization accuracy, achieved with simulated and experimentally recorded data, proved comparable in the range of E_d (Fig. 7, for 5-MMs tracking). For instance, with 5-MMs, the averaged $\bar{E}_d$ retrieved in the simulations proved 0.6 mm and 0.12 mm (at the localization rates of 20 and 100 Hz, respectively), versus 2.6 mm and 0.12 mm, achieved with the experimental setup. In addition, the results from the experimental setup proved consistent (and comparable) with the unimodal/bimodal feature observed for different localization rates.

IV. Discussion

In this work, we simulated the effects of the intrinsic properties of magnetic field sensors on the localization accuracy and computation time in a multi-magnet localization scenario.

While previous studies focussed on the number, arrangement and noise of the sensors [13], [18], [21], [28], here we aimed to investigate complementary issues, not investigated yet, i.e., the sensor resolution and localization rate.

Moreover, aiming to effectively translate the proposed localization method into the myokinetic interface, we also explored a higher number of MMs compared to previous investigations. In particular, by systematically varying the number of MMs to track, $L_{MM-sensor}$, sensor resolution and localization rate, we aimed at identifying general and effective guidelines for the design of multi-DoF magnetic tracking systems operating in similar workspaces. We assessed the localization accuracy using E_d, [14], [15], [18] and validated the simulated results by means of an experimental test with a physical system (Fig. 3). Concerning the relationship between $\bar{E}_d$ and $L_{MM-sensor}$ (Fig. 4a), we argue that this was due to the combined effect of two opposite phenomena: the approximations in the dipole model for small distances, and the signal-to-noise ratio of the readings (SNR) for large distances. In particular, it is known that the accuracy of the point-dipole model increases with the distance, or in other words, E_d decreases with $L_{MM-sensor}$ [15], [16]. Conversely, the SNR, which decreases with the distance, likely yielded to the increase of the E_d for larger values of $L_{MM-sensor}$. This might also explain why coarser resolutions (enhancing $\bar{E}_d$) shifted the minimum of the parabola towards the left, i.e., towards smaller values of $L_{MM-sensor}$.

Moreover, although other studies described this relationship with a monotonic trend [15], [16], [34], [35], our outcomes agree with those experimentally assessed by our group [29]. The same behaviour was found independently of the localization rate, except for the only value of $L_{MM-sensor} = 10$ mm and number of MMs greater than 4 (Fig. 4b). Since the field values were generated through an analytical model [31], we argue that this behaviour was again caused by the simplifications in the dipole model used for tracking. Hence, similar errors could be likely found with a physical system.

The fact that the variability of the lobes of E_d increases for coarser values of resolution is not a surprise (Fig. 5). Interestingly, the distributions of E_d switched from bimodal to unimodal for localization rates greater than a value in the 80-100 Hz interval. This was mainly caused by swapped neighbouring MMs, or neighbouring MMs mislocalized in between their actual positions. Hence, apparently, beyond 100 Hz (or $d < 1$ mm) the cost function of the LMA could be better minimized. In other words, the bimodality of the distribution suggests that for localization rates too low w.r.t. the speed of the travelling MMs, the localization is not accurate. Unexpectedly, this effect could not be attenuated by better resolutions, but only by better localization rates. This suggests that when choosing a sensor for magnetic tracking, the selection should favour high sampling frequencies over absolute accuracy. Such statement is even more true given that the coarsest resolution simulated (10 mG) was deliberately overestimated and is rarely retrieved in the market. Nevertheless, we argue that considering such a poor resolution proved informative to describe realistic situations affected by environmental noises and interferences.

To obtain insights into a multi-objective tracker that are also functional to subsequent hardware implementations, we investigated the effects of the sensor resolution and localization rate on the solver computation time (Fig. 6). The cost of the localization is usually evaluated in terms of computation time by a specific/used hardware [6], [8], [15], [18], [29]. By contrast, in this study we considered the number of iterations needed by the solver to converge, which is software, rather than hardware dependent. In other words, this produced results which are specific to the LMA, and do not rely on the computation capability of a specific hardware. The number of iterations of the solver, i_N, proved independent on the resolution (Fig. 6a). Hence, in the resolution range explored, the SNR was evidently always very high. In other words, sensors retained enough information to introduce negligible influences on the quality of tracking. This is reasonable, considering that the decimation of the least significant digits of the readings may have an impact on the gradient (slope) of the cost function, but not on its overall structure.

Our approach allowed us to achieve quite generalizable results, but at the same time, it prevented us from drawing conclusions specific to a certain hardware or application. First, a planar distribution was used for both the sensors and the MMs. This approach was supported by the fact that previous investigations based on the same planar geometry [20] could be effectively translated to a curved, more realistic geometry [36]. Related to this, while the grid of 600 sensors appears technically complex (in terms of wiring, computing units, temporal delays, power consumption, etc.), studying it, allowed us to decouple the impact of resolution from the one of sensor placement, which has already been studied [21], [28]. In this sense, it represents an important asset of our study, which aimed at identifying general rules, not specific to the hardware choice. Nonetheless, the technical complexity could be significantly reduced without losing performance; as a fact, previous studies suggest that magnetic tracking is more affected by the sensor placement than by its number [26], [36].

Secondly, to limit the number of combinations tested, as well as to have better control over the parameters under study (i.e., $L_{MM-sensor}$, resolution, localization rate, and number of MMs), the orientation of the MMs was kept fixed. This prevents us from drawing conclusions on the magnitude of the orientation error, when MMs are left free to rotate. Thirdly, the effects of external interferences or sensor saturation and hysteresis were not considered. This allowed us to keep the results general (i.e., again, not specific to a certain hardware/environment). However, while the external disturbances could be potentially characterized and then rejected/filtered or shielded, sensor saturation and hysteresis are less predictable. Hence, we invite further studies in which these factors are considered. Nonetheless, based on our experience and considering MMs and sensors similar to those used in this study, sensor saturation (and thus hysteresis) may apply only when the $L_{MM-sensor}$ is below $\sim$20 mm.

To conclude, this study suggests that the accuracy of a multi-objective magnetic tracker can be improved by increasing its localization rate, rather than its sensing resolution. Accordingly, when designing the sensing apparatus, high sampling frequency sensors and electronic architectures, maximising the data throughput, should be chosen.

REFERENCES

[1] K. Cleary and T. M. Peters, "Image-guided interventions: Technology review and clinical applications," *Annu. Rev. Biomed. Eng.*, vol. 12, no. 1, pp. 119–142, Jul. 2010.

[2] A. M. Franz *et al.*, "Electromagnetic tracking in medicine—A review of technology, validation, and applications," *IEEE Trans. Med. Imag.*, vol. 33, no. 8, pp. 1702–1725, Aug. 2014.

[3] T. Langerak, J. J. Zárate, D. Lindlbauer, C. Holz, and O. Hilliges, "Omni: Volumetric sensing and actuation of passive magnetic tools for dynamic haptic feedback," in *Proc. 33rd Annu. ACM Symp. User Interface Softw. Technol.*, 2020, pp. 594–606.

[4] K.-Y. Chen, S. N. Patel, and S. Keller, "Finexus: Tracking precise motions of multiple fingertips using magnetic sensing," in *Proc. CHI Conf. Hum. Factors Comput. Syst.*, May 2016, pp. 1504–1514.

[5] M. Salerno, R. Rizzo, E. Sinibaldi, and A. Menciassi, "Force calculation for localized magnetic driven capsule endoscopes," in *Proc. IEEE Int. Conf. Robot. Autom.*, May 2013, pp. 5354–5359.

[6] C. Hu *et al.*, "Locating intra-body capsule object by three-magnet sensing system," *IEEE Sensors J.*, vol. 16, no. 13, pp. 5167–5176, Jul. 2016.

[7] A. Z. Taddese, P. R. Slawinski, M. Pirotta, E. De Momi, K. L. Obstein, and P. Valdastri, "Enhanced real-time pose estimation for closed-loop robotic manipulation of magnetically actuated capsule endoscopes," *Int. J. Robot. Res.*, vol. 37, no. 8, pp. 890–911, Jul. 2018.

[8] D. Son, X. Dong, and M. Sitti, "A simultaneous calibration method for magnetic robot localization and actuation systems," *IEEE Trans. Robot.*, vol. 35, no. 2, pp. 343–352, Apr. 2019.

[9] Z. Sun, L. Maréchal, and S. Foong, "Passive magnetic-based localization for precise untethered medical instrument tracking," *Comput. Methods Programs Biomed.*, vol. 156, pp. 151–161, Mar. 2018.

[10] S. Krueger, H. Timinger, R. Grewer, and J. Borgert, "Modality-integrated magnetic catheter tracking for X-ray vascular interventions," *Phys. Med. Biol.*, vol. 50, no. 4, p. 581, 2005.

[11] J. Edelmann, A. J. Petruska, and B. J. Nelson, "Magnetic control of continuum devices," *Int. J. Robot. Res.*, vol. 36, no. 1, pp. 68–85, 2017.

[12] S. M. Cromer Berman, P. Walczak, and J. W. M. Bulte, "Tracking stem cells using magnetic nanoparticles," *Wiley Interdiscipl. Rev., Nanomed. Nanobiotechnol.*, vol. 3, no. 4, pp. 343–355, Jul. 2011.

[13] S. Tarantino, F. Clemente, D. Barone, M. Controzzi, and C. Cipriani, "The myokinetic control interface: Tracking implanted magnets as a means for prosthetic control," *Sci. Rep.*, vol. 7, no. 1, Dec. 2017, Art. no. 17149.

[14] W. Yang, C. Hu, M. Li, M. Q.-H. Meng, and S. Song, "A new tracking system for three magnetic objectives," *IEEE Trans. Magn.*, vol. 46, no. 12, pp. 4023–4029, Dec. 2010.

[15] C. R. Taylor, H. G. Abramson, and H. M. Herr, "Low-latency tracking of multiple permanent magnets," *IEEE Sensors J.*, vol. 19, no. 23, pp. 11458–11468, Aug. 2019.

[16] S. Tarantino, F. Clemente, A. De Simone, and C. Cipriani, "Feasibility of tracking multiple implanted magnets with a myokinetic control interface: Simulation and experimental evidence based on the point dipole model," *IEEE Trans. Biomed. Eng.*, vol. 67, no. 5, pp. 1282–1292, May 2020.

[17] D. J. Griffiths, *Introduction to Electrodynamics*, vol. 2. Cambridge, U.K.: Cambridge Univ. Press, 2017.

[18] C. Hu, M. Q.-H. Meng, and M. Mandal, "Efficient linear algorithm for magnetic localization and orientation in capsule endoscopy," in *Proc. IEEE Eng. Med. Biol. 27th Annu. Conf.*, Jan. 2005, pp. 7143–7146.

[19] S. Yabukami *et al.*, "Motion capture system of magnetic markers using three-axial magnetic field sensor," *IEEE Trans. Magn.*, vol. 36, no. 5, pp. 3646–3648, Sep. 2000.

[20] M. Gherardini, F. Clemente, S. Milici, and C. Cipriani, "Localization accuracy of multiple magnets in a myokinetic control interface," *Sci. Rep.*, vol. 11, no. 1, Dec. 2021, Art. no. 4850.

[21] C. Hu, T. Ma, and M. Q.-H. Meng, "Sensor arrangement optimization of magnetic localization and orientation system," in *Proc. IEEE Int. Conf. Integr. Technol.*, Mar. 2007, pp. 311–315.

[22] A. J. Petruska and J. J. Abbott, "Optimal permanent-magnet geometries for dipole field approximation," *IEEE Trans. Magn.*, vol. 49, no. 2, pp. 811–819, Feb. 2013.

[23] J. Montero, M. Gherardini, F. Clemente, and C. Cipriani, "Comparison of online algorithms for the tracking of multiple magnetic targets in a myokinetic control interface," in *Proc. IEEE Int. Conf. Robot. Autom. (ICRA)*, May 2020, pp. 2770–2776.

[24] K. Yu, G. Fang, and E. Dutkiewicz, "Position and orientation accuracy analysis for wireless endoscope magnetic field based localization system design," in *Proc. IEEE Wireless Commun. Netw. Conf.*, Apr. 2010, pp. 1–6.

[25] V. Pasku *et al.*, "Magnetic field-based positioning systems," *IEEE Commun. Surveys Tuts.*, vol. 19, no. 3, pp. 2003–2017, 3rd Quart., 2017.

[26] L. Maréchal, S. Foong, S. Ding, K. L. Wood, V. Patil, and R. Gupta, "Design optimization of a magnetic field-based localization device for enhanced ventriculostomy," *J. Med. Devices*, vol. 10, no. 1, pp. 1–9, Mar. 2016.

[27] S. Foong, K.-M. Lee, and K. Bai, "Harnessing embedded magnetic fields for angular sensing with nanodegree accuracy," *IEEE/ASME Trans. Mechatronics*, vol. 17, no. 4, pp. 687–696, Aug. 2012.

[28] O. Talcoth and T. Rylander, "Optimization of sensor positions in magnetic tracking," Chalmers Univ. Technol., Gothenburg, Sweden, Tech. Rep., 2011.

[29] F. Clemente, V. Ianniciello, M. Gherardini, and C. Cipriani, "Development of an embedded myokinetic prosthetic hand controller," *Sensors*, vol. 19, no. 14, p. 3137, Jul. 2019.

[30] Y. Higuchi, T. Nara, and S. Ando, "Complete set of partial differential equations for direct localization of a magnetic dipole," *IEEE Trans. Magn.*, vol. 52, no. 5, May 2016, Art. no. 4000910.

[31] N. Derby and S. Olbert, "Cylindrical magnets and ideal solenoids," *Amer. Phys.*, vol. 78, no. 3, pp. 229–235, 2010.

[32] J. Nocedal and S. Wright, *Numerical Optimization*. Berlin, Germany: Springer, 2006.

[33] Á. Jobbágy, P. Harcos, R. Karoly, and G. Fazekas, "Analysis of finger-tapping movement," *J. Neurosci. Methods*, vol. 141, no. 1, pp. 29–39, Jan. 2005.

[34] V. Schlageter, P.-A. Besse, R. Popovic, and P. Kucera, "Tracking system with five degrees of freedom using a 2D-array of Hall sensors and a permanent magnet," *Sens. Actuators A, Phys.*, vol. 92, no. 1, pp. 37–42, Aug. 2001.

[35] S. Su *et al.*, "Investigation of the relationship between tracking accuracy and tracking distance of a novel magnetic tracking system," *IEEE Sensors J.*, vol. 17, no. 15, pp. 4928–4937, Aug. 2017.

[36] S. Milici, M. Gherardini, F. Clemente, F. Masiero, P. Sassu, and C. Cipriani, "The myokinetic control interface: How many magnets can be implanted in an amputated forearm? Evidence from a simulated environment," *IEEE Trans. Neural Syst. Rehabil. Eng.*, vol. 28, no. 11, pp. 2451–2458, Nov. 2020.

Federico Masiero received the B.Sc. degree in information engineering from the University of Padua, Padua, Italy, in 2017, and the M.Sc. degree in bionics engineering from the University of Pisa and Scuola Superiore Sant'Anna, Pisa, Italy, in 2019. He is currently pursuing the Ph.D. degree in biorobotics at The BioRobotics Institute, Scuola Superiore Sant'Anna, Pisa, where he is involved in national and European research projects. His research interests mainly include the modeling and development of electro-magnetic systems and devices for prosthetics and rehabilitation robotics.

Edoardo Sinibaldi (Member, IEEE) received the B.Sc./M.Sc. (Hons.) degrees in aerospace engineering from the University of Pisa, Italy, in 2002, after an internship at Rolls-Royce plc, Derby, U.K., during which he studied computational geometry methods for air-breathing engines applications, and the Ph.D. (Hons.) degree in mathematics for technology and industry from the Scuola Normale Superiore, Pisa, where he developed numerical methods for computational fluid dynamics. After a postdoctoral period at The BioRobotics Institute, Scuola Superiore Sant'Anna, Pisa, mainly addressing competitive fundraising and project technical management, he moved to the Italian Institute of Technology (IIT). His research activity bridges modeling (at large, and particularly for biomedical applications), model-based design (particularly for flexible tools), and bioinspired soft robotics (at large, and particularly bioinspired actuation). He is currently serving as the Editorial Board Member (an Associate/an Academic Editor) for PLOS ONE, the *International Journal of Advanced Robotic Systems*, and *Scientific Reports* (Nature Research).

Francesco Clemente received the M.Sc. degree in biomedical engineering from the University of Pisa, Italy, in 2012, and the Ph.D. degree in biorobotics from Scuola Superiore Sant'Anna, Pisa, Italy, in 2016. In Scuola Superiore Sant'Anna, he worked on several national and international projects, dealing with the design and development of sensory feedback devices as well as control algorithms for upper limb prostheses. After being appointed as an Assistant Professor for three years, he moved to the private sector in 2020. He is now the Managing Director of Prensilia SRL, a spin-off company of Scuola Superiore Sant'Anna commercializing robotic hands for clinical and research purpose.

Christian Cipriani (Senior Member, IEEE) received the M.Sc. degree in electronic engineering from the University of Pisa, Pisa, Italy, in 2004, and the Ph.D. degree in biorobotics from the IMT Institute for Advanced Studies, Lucca, Italy, in 2008. He is currently the Director of The BioRobotics Institute, Scuola Superiore Sant'Anna, Pisa, where he is also a Professor of Bioengineering and the Head of the Artificial Hands Area. He is the Coordinator and PI of the MYKI Project (H2020 ERC 679820) and the DeTOP Project (H2020 ICT 687905). He has coordinated several national and international research projects and authored over 150 peer-reviewed scientific papers, 90 of which were in international journals. He was a Visiting Scientist with the University of Colorado, Denver | Anschutz Medical Campus, in 2012. He founded a spin-off company in 2009. His research interests cover mechatronic, controllability, and sensory feedback issues of dexterous robotic hands to be used as thought-controlled prostheses. Dr. Cipriani is a recipient of several awards, including a Starting Grant from the European Research Council in 2015, an early career grant by the Italian Ministry of Research in 2011 (FIRB 2010 Program), a Fulbright Research Scholar Fellowship in 2011, and the d'Auria Award from the Italian Robotics and Automation Association in 2009. He is a Senior Member of the IEEE Robotics and Automation Society and the IEEE Engineering in Medicine and Biology Society.